Accepted Manuscript

Title: Tailoring the supramolecular structure of amphiphilic glycopolypeptide analogue toward liver targeted drug delivery systems

Authors: Aisha Roshan Mohamed Wali, Jie Zhou, Shengnan Ma, Yiyan He, Dong Yue, James Zhenggui Tang, Zhongwei Gu

PII: S0378-5173(17)30289-2
DOI: http://dx.doi.org/doi:10.1016/j.ijpharm.2017.04.009
Reference: IJP 16574

To appear in: *International Journal of Pharmaceutics*

Received date: 6-12-2016
Revised date: 30-3-2017
Accepted date: 4-4-2017

Please cite this article as: Wali, Aisha Roshan Mohamed, Zhou, Jie, Ma, Shengnan, He, Yiyan, Yue, Dong, Tang, James Zhenggui, Gu, Zhongwei, Tailoring the supramolecular structure of amphiphilic glycopolypeptide analogue toward liver targeted drug delivery systems.International Journal of Pharmaceutics http://dx.doi.org/10.1016/j.ijpharm.2017.04.009

Tailoring the supramolecular structure of amphiphilic glycopolypeptide analogue toward liver targeted drug delivery systems

Aisha Roshan Mohamed Wali[b,1], Jie Zhou[a,1], Shengnan Ma[a], Yiyan He[a,c,*], Dong Yue[a], James Zhenggui Tang[b] and Zhongwei Gu[a,c,*]

[1] Aisha Roshan Mohamed Wali and Jie Zhou contributed equally to this work

[a] National Engineering Research Center for Biomaterials, Sichuan University, No. 29, Wangjiang Road, Chengdu 610065, Sichuan, P. R. China

[b] School of Pharmacy, Faculty of Science and Engineering, University of Wolverhampton, Wulfruna Street, Wolverhampton WV1 1LY, United Kingdom

[c] College of Materials Science and Engineering, Nanjing Tech University, 30 South Puzhu Road, Nanjing 211816, P. R. China.

* Corresponding authors: heyiyan2005@163.com (Yiyan He); zwgu1006@hotmail.com & zwgu@scu.edu.cn (Zhongwei Gu)

Graphic Abstract

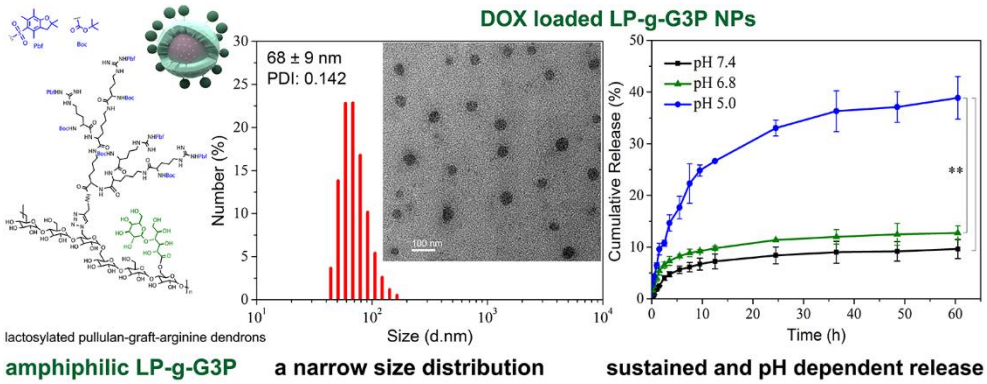

Abstract:

Amphiphilic glycopolypeptide analogues have harboured great importance in the development of targeted drug delivery systems. In this study, lactosylated pullulan-graft-arginine dendrons (LP-g-G3P) was synthesized using Huisgen azide-alkyne 1,3-dipolar cycloaddition between lactosylated pullulan and generation 3 arginine dendrons bearing Pbf and Boc groups on the periphery. Hydrophilic lactosylated pullulan was selected for amphiphilic modification, aiming at specific lectin recognition. Macromolecular structure of LP-g-G3P combined alkyl, aromatic, and peptide dendritic hydrophobic moieties and was able to self-assemble spontaneously into core-shell nanoarchitectures with small particle sizes and low polydispersity in the aqueous media, which was confirmed by CAC, DLS and TEM. Furthermore, the polyaromatic anticancer drug (doxorubicin, DOX) was selectively encapsulated in the hydrophobic core through multiple interactions with the dendrons, including π-π interactions, hydrogen bonding and hydrophobic interactions. Such multiple interactions had the merits of enhanced drug loading capacity (16.89 ± 2.41%), good stability against dilution, and excellent sustained release property. The cell viability assay presented that LP-g-G3P nanoparticles had an excellent biocompatibility both in the normal and tumor cells. Moreover, LP-g-G3P/DOX nanoparticles could be effectively internalized into the hepatoma carcinoma cells and dramatically inhibited cell proliferation. Thus, this approach

paves the way to develop amphiphilic and biofunctional glycopolypeptide-based drug delivery systems.

Keywords: amphiphilic polysaccharide, peptide dendrons, glycopolypeptide, sustained release, targeted drug delivery

1. Introduction

Biological organisms, such as cells, were generated from precise self-assembly of natural carbohydrates, nucleic acids, and amino acids (Carlini et al., 2016). The self-assembly of amphiphilic molecules in a selective solvent also gives a versatile way to produce highly organized, well-defined micellar or vesicular nanostructures (Börner, 2009; Qiu et al., 2015; Wang et al., 2012). Numerous approaches have been developed for the self-assembly of natural or synthetic amphiphiles into soft core-shell nanoobjects which are of great interest in the field of drug delivery systems, wherein the hydrophobic nature of the micellar core can provide a safe harbor for hydrophobic drugs and the hydrophilic shell protects the core from an aqueous environment (Rösler et al., 2012). Among these amphiphilic molecules, amphiphiles containing natural blocks, such as polysaccharides or polypeptides, have attracted the most attention because they are non-toxic, non-immunogenic, biocompatible, biodegradable, and renewable (Akhlaghi et al., 2013; Hassani et al., 2012). Nanostructures obtained from the self-assembly of natural blocks are expected to have great potential in the development of biomedical applications, in particular, as nanocarriers for the delivery of drugs, proteins and genes. For example, polysaccharides-based amphiphilic polymers are the subjects of many studies (Alvarez-Lorenzo et al., 2013; Hassani et al., 2012; Saravanakumar et al., 2012) with the purpose of delivering hydrophobic anticancer drugs.

Polysaccharides, such as chitosan, dextran, pullulan, hyaluronic acid, heparin, and alginic acid, have a wide range of molecular weight and a large number of reactive groups (-COOH, -NH_2, -OH, etc.). Therefore, polysaccharides can be easily chemically modified to be various

amphiphilic derivatives (Akhlaghi et al., 2013; Hassani et al., 2012; Liu et al., 2011). Current hydrophobic moieties involved in creating amphiphilic polysaccharides derivatives that undergo self-assembly in aqueous solutions include linear molecules (long-chain fatty acids (Nichifor et al., 2014; Pramod et al., 2012) and poly(ε-caprolactone) (Chandel et al., 2016; Gu et al., 2014)), cyclic molecules (cholesterol (Kawasaki et al., 2016; Takahashi et al., 2011), bile acids (Li et al., 2012), and doxorubicin (Cao et al., 2010; Xu et al., 2015)), polyacrylate family (Poly(methyl methacrylate) (Dupayage et al., 2011; Dupayage et al., 2008) and poly(isobutyl cyanoacrylate) (Bravo-Osuna et al., 2007; Wang et al., 2011)), etc. The stability and polarity of amphiphilic polysaccharides based nanostructures are closely related to structural characteristics of amphiphiles, such as hydrophobicity and intra- /intermolecular interactions (Aschenbrenner et al., 2013). A promising alternative strategy for the generation of amphiphilic derivatives is to study the use of dendritic molecules (Hassan et al., 2004; Percec et al., 2004), such as peptide dendritic molecules (Li et al., 2013), mainly due to the unique radiate dendritic structures, low polydispersity and the amplification effect, which can be harnessed for providing large void space within the hydrophobic inner core. Generally, dendrons involving well-defined molecular structures allow multivalency in a tunable way upon selecting the peripheral chemical groups and the generation properly (Majoinen et al., 2014; Roglin et al., 2011; Rosen et al., 2009). However, the number of hydrophobically modified polysaccharides based systems that have been thoroughly investigated is limited and among existing studies only a few contain information about combination use of different types of hydrophobic molecules. Therefore, it provides us ample opportunities to modify polysaccharides hydrophobically with fine-tuned properties for drug delivery.

Herein, we present a straightforward and versatile synthesis of a glycopolypeptide analogue, amphiphilic polysaccharide-based graft copolymer, in which hydrophobic polypeptide blocks are covalently attached to a hydrophilic polysaccharide block. Macromolecular structures of this type combine alkyl, aromatic, and peptide dendritic hydrophobic moieties and are able to self-assemble spontaneously into core-shell nanocarriers in water by the fine-tuning of intra- and intermolecular

interactions. As a proof of concept, we illustrate the synthesis of lactosylated pullulan-graft-arginine dendrons (LP-g-G3P) based on the conjugation of lactosylated pullulan with generation 3 arginine dendrons bearing Pbf and Boc groups on the periphery through Huisgen azide-alkyne 1,3-dipolar cycloaddition or "click" reaction. In this study, a hydrophilic polysaccharide derivative, lactosylated pullulan, was selected for hydrophobic modification. Pullulan is a neutral linear polysaccharide composed of α-(1-6)-linked maltotriosyl repeating units. The attractive properties of both lactose and pullulan not only lie in their water-solubility, biocompatibility, and non-immunogenicity, but also the higher affinity toward liver due to the presence of lectin like receptors on liver cells (hepatocytes and Kupffer cells), which possess biological affinity for sugar residues (Kawasaki et al., 2016; Singh et al., 2015). Harnessing these merits of pullulan and lactose in constructing amphiphilic blocks could be of great benefit for the development of liver targeted drug delivery systems.

Acronyms

Alkyne-G1(K)P: alkyne-generation 1 (G1) lysine dendron bearing protecting groups

Alkyne-G2(K)P: alkyne-generation 2 (G2) lysine dendron bearing protecting groups

Alkyne-G3(R)P: alkyne-generation 3 (G3) arginine dendron bearing protecting groups

Azido-P: azidated pullulan

Azido-LP: azido-lactosylated pullulan

LP-g-G3P: lactosylated pullulan graft G3(R)P

2. Materials and methods

2.1. Materials

2-Propynylamine was purchased from J&K Company. Boc-L-Arg(Pbf)-OH, Boc-L-Lys(Boc)-OH, N-(3-dimethylaminopropyl)-N’-ethylcarbodiimide hydrochloride (EDCI), 1-hydroxybenzotriazole hydrate (HOBt) and O-Benzotriazole-N,N,N’,N’-tetramethyl-uronium-hexafluoro-phosphate (HBTU) were commercially available from GL Biochem Ltd (Shanghai, China), where Pbf denotes 2,2,4,6,7-pentamethyldihydrobenzofuran-5-sulfonyl, Boc denotes

tertiary-butyloxycarbonyl. Sodium azide (NaN_3), triphenylphosphine (PPh_3), tetrabromethane (CBr_4), 4-Dimethylaminopyridine (DMAP), copper sulfate pentahydrate ($CuSO_4 \cdot 5H_2O$), sodium ascorbate (SA), pullulan (MW 20,000 Da), triethylamine (TEA), ethylenediaminetetraacetic acid disodium salt (EDTA·2Na) and lactobionic acid were commercially purchased from Aladdin® Ltd. Trifluoroacetic acid (TFA), N, N-diisopropylethylamine (DIEA), sodium chloride (NaCl), hydrochloric acid (HCl), anhydrous magnesium sulfate ($MgSO_4$) and sodium bicarbonate ($NaHCO_3$) were ordered from Asta Tech Pharmaceutical (Chengdu, China). Doxorubicin hydrochloride (DOX·HCl) was purchased from Zhejiang Hisun Pharmaceutical. Regenerated Cellulose Dialysis Membranes (MWCO = 100-500, 1000 and 3500 Da) were obtained from Spectrum/Por (Houston, USA). The human liver hepatocellular carcinoma cell line (HepG2) and mouse embryonic fibroblast cell line (NIH3T3) were obtained from Shanghai Institutes for Biological Sciences (China). Dulbecco's modified Eagle's medium with high glucose (DMEM-HG) and fetal bovine serum (FBS) were from Life Technologies Corporation (Gibco®, USA). A Cell-Counting Kit-8 (CCK-8) was obtained from Dojindo Laboratories (Tokyo, Japan). PBS buffer and other buffers were prepared in MilliQ ultrapure water and filtered (0.22 μm) prior to use, and all other chemicals were ordered from Aldrich and used as received.

2.2. Synthesis of alkyne-G3(R)P

The alkynyl peptide dendrons were prepared using the previously reported methods (Li et al., 2013; Luo et al., 2012) with a few modifications. Firstly, Boc-Lys(Boc)-OH (3.50 g, 1.10 mmol), HOBt (1.30 g, 1.10 mmol) and EDCI (2.00 g, 1.10 mmol) were co-dissolved into 40.00 mL of dried DCM under N_2 atmosphere. The flask was kept under ice bath and DIEA (6.30 mL, 4.00 mmol) was injected into the mixture followed by the addition of propargylamine (0.60 mL, 1.00 mmol). The mixture was first stirred at 0°C for 30 min and then brought at room temperature for 48 hours. Purification of the product was done by washing process and separation by column chromatography: after the reaction, the mixture was concentrated by removing DCM through rotary evaporation and then dissolved with 300.00 mL of chloroform. Impurities (amines or

unwanted acids) from the organic solution were removed by a three-time repeat of basic, acid and a brine wash with saturated $NaHCO_3$, HCl (1 M) and NaCl. After the washing process, the organic phase was dried overnight with a decent amount of drying agent ($MgSO_4$). The organic phase was lastly collected by a standard filtration method and again concentrated by rotary evaporation. Further purification was carried out by column chromatography using ethyl acetate/petroleum ether (1/1, V/V) as an eluent. The final purified product obtained was dried by rotary evaporation, then by low-pressure pump followed with vacuum drying to obtain a white solid of alkyne-G1(K)P (2.60 g, 74.01%).

For the preparation of alkyne-G2(K)P, amino deprotection of alkyne-G1(K)P was conducted to give cationic alkyne-G1(K). Alkyne-G1(K)P (2.60 g, 1.00 mmol) was stirred in 16.00 mL of anhydrous TFA and DCM mixture (1.8/1, V/V) for 5 hours at room temperature under N_2 atmosphere. After the solvent was removed by rotary evaporation, absolute diethyl ether was added and the precipitates were then collected and dried under high vacuum. Thin-Layer Chromatography (TLC) was used to monitor if all the Boc groups were removed. Alkyne-G2(K)P was then prepared by co-dissolving an equal molar of Boc-Lys(Boc)-OH (3.50 g, 2.40 mmol), HOBt (1.30 g, 2.40 mmol), HBTU (2.00 g, 2.40 mmol) and alkyne-G1(K) (0.383g, 1.00 mmol) into 50.00 mL of dried DMF under N_2 atmosphere. DIEA (6.00 mL, 5.00 mmol) was added and the mixture was stirred at room temperature for 48 hours. The pure product was obtained by using the same method used to purify alkyne-G1(K)P. Washing with saturated $NaHCO_3$, HCl (1 M) and NaCl was carried out with a repeat of 3 times each. The obtained crude product of alkyne-G2(K)P was then purified by column chromatography (ethyl acetate /petroleum ether = 4/1, V/V) and the obtained yield was of 12.5g, 78.02%.

Amino deprotection of alkyne-G2(K)P was conducted by the same procedure as described for alkyne-G1(K)P. The obtained alkyne-G2(K)P (1.00 mmol) was treated with 7.00 mL of anhydrous TFA (40.00 mmol)/DCM mixture (1.8/1, V/V) and stirred for 8 hours at room temperature under N_2 atmosphere. White product of alkyne-G2(K) (6.30 g) was obtained after

precipitation with absolute diethyl ether. The synthesis of alkyne-G3(R)P was then carried out by co-dissolving an equal molar of Boc-Arg(pbf)-OH (12.00 g, 6.00 mmol), HOBt (3.30 g, 6.00 mmol) and HBTU (8.79 g, 6.00 mmol) and alkyne-G2(K) (1.70 g, 1.00 mmol) into 55.00 mL of dried DMF under N_2 atmosphere. DIEA (6.00 mL, 5.00 mmol) was added and then the mixture was stirred at room temperature for 48 hours. Purification was similar to that of alkyne-G1(K)P and alkyne-G2(K)P using ethyl acetate/petroleum ether (40/1, V/V) followed by the use of DCM/methanol (10/1, V/V) as eluents. The yield of the final hydrophobic alkyne-G3(R)P was 7.00 g, 73.20 %.

2.3. Synthesis of azido-LP

A typical azido-P synthetic procedure was shown as follows: firstly, pullulan (1.00 g, 1.00 mmol, equivalent of anhydrous glucoside units) and NaN_3 (3.90 g, 10.00 mmol) were added into a 100 mL flask. 30 mL of anhydrous DMF was then injected and the mixture was stirred at 80°C for 2 hours under N_2 atmosphere to completely dissolve pullulan. After cooling to room temperature, ice bath was added in one flask and the other flask was left at room temperature. Freshly prepared solution of PPh_3 (2.00 g, 1.60 mmol) in 5.00 mL of DMF into the flask was added followed by an addition of a solution of CBr_4 (3.00 g, 1.60 mmol) in 5.00 mL of DMF and the solution turned to dark yellow colour. The ice bath was removed after 30 min of stirring and both reactions was allowed to stir for 20 hours at RT. The reaction process carried out in ice bath was repeated with a molar ratio of 1:8 or 1:9 (pullulan: NaN_3). After 20 hours of stirring, the solution was left exposed to air and methanol (5.00 mL) was added to quench the reaction. The azido-P was precipitated in 300.00 mL of ethanol. Finally, the precipitate was recovered by centrifugation and washing with 100.00 mL of a 7:3 ethanol/water (V/V) solution followed by ethanol. The solid obtained was then allowed to dry at 60°C overnight in vacuum. A yield of 0.90 g was obtained.

Conjugation of lactobionic acid into azido-P (azido-LP) was synthesized by condensing the carboxyl group of lactobionic acid and the hydroxyl group of pullulan. Firstly, azido-P (0.77 g, 1.00 mmol equivalent of anhydrous glucoside units) was added in 20 mL of anhydrous DMSO and

the mixture was magnetically stirred at 60°C for 2 hours to achieve a complete dissolution. Separately, activation of the carboxyl groups was carried out by dissolving lactobionic acid (10.50 g, 8.00 mmol), EDCI (3.80 g, 5.40 mmol) as the ester-activator intermediate and DMAP (2.24 g, 5.00 mmol) as the catalyst in 40.00 mL of anhydrous DMSO at 50-60°C under N_2 atmosphere. To this solution, the azido-P solution was then added dropwise and the resulting dark brown mixture was stirred for 48 hours at 60°C. Purification was achieved by dropping the mixture into 90% of ethanol (300.00 mL) under vigorously stirring and then the precipitated product was dialyzed against DI water (MWCO 3500 Da) for 1 day. The brown solids appeared in the dialysis bag were then collected by lyophilisation.

2.4. Synthesis of LP-g-G3P

Click reaction was carried out between azido-LP and alkyne-G3(R)P. Alkyne-G3(R)P (2.35 g, 2.00 mmol) and azido-LP (0.10 g, 1.00 mmol) were added successively in 30.00 mL DMSO and the mixture was stirred to dissolve under N_2 atmosphere at 50°C for 1 hour. The mixture was then brought at room temperature and passed into argon, then 5.00 mL of deoxygenised aqueous solution of sodium L-ascorbate (0.08 g, 0.40 mmol) and 5.00 mL of blue aqueous solution of copper (II) sulphate pentahydrate (0.05 g, 0.20 mmol) were added successively into the reaction. The yellowish resultant mixture was stirred for 55 hours. Light and any trace of oxygen were avoided during the reaction period to prevent any oxidation of the copper ions or de-activation of the sodium L-ascorbate. After the reaction, a little amount of EDTA·2Na was added and the mixture was stirred for 2-3 hours until the solution turned blue in the presence of air. The resulting solution was finally dialysed against DI water for 2 days (MWCO 3500 Da) and then lyophilized to yield the product LP-g-G3P.

2.5. Characterisation Techniques

The structures of alkyne-G1(K)P, alkyne-G2(K)P and alkyne-G3(R)P were confirmed by Mass Spectrum (MS). ^{1}H-nuclear magnetic resonance (^{1}H-NMR) analysis was carried out using a Bruker advanced 400 nuclear magnetic resonance spectrometer. The samples were dissolved in

DMSO-d_6 or D_2O before the measurements. The pullulan derivatives were characterised by Fourier Transform Infrared Spectroscopy (FTIR) and ^{1}H-NMR.

2.6. (Critical Association Concentration) CAC studies

The critical association concentration was studied by fluorescence spectroscopy using pyrene as a hydrophobic fluorescence dye. Triplicate solutions of pyrene mixed with LP-g-G3P nanoparticles of varying concentrations (1×10^{-5} to 0.1 mg/mL) were prepared, of which the concentration in each sample solution was 6.0×10^{-7} mol/L. Fluorescence emission spectra of pyrene was obtained by exciting samples at 390 nm and intensities at 337 nm and 334 nm were recorded. All fluorescence measurements were carried out at 25.0 ± 0.1°C in the absence of light. The CAC value was determined by plotting a curve of the intensity ratio (I_{337}/I_{334}) against the Log of LP-g-G3P concentrations (mg/mL) where the correspondent CAC value was the crossover point when extrapolating the intensity ratio (I_{337}/I_{334}) at low and high concentration regions.

2.7. Preparation of DOX-encapsulated nanoparticles

The blank nanoparticles of LP-g-G3P were prepared by dissolving 5.00 mg of LP-g-G3P in 1.00 mL of DMSO and then dropping into 5.00 mL of deionized water under vigorously stirring followed by the analysis or freezing. For the preparation of drug loaded nanoparticles, LP-g-G3P in DMSO (5.00 mg/mL) was added in 1.00 mL of hydrophobic doxorubicin (DOX, 6.00 mg/mL) solution and dispersed into 10.00 mL of deionized water under stirring. The mixture obtained was then dialysed against water for 24 hours to remove unloaded drug (6 changes of water/day) using a MWCO 3500 Da dialysis membrane and the resultant solution was then analysed or freeze dried.

The loading content of DOX was calculated by fluorescence measurement (F-7000, excitation at 480 nm) in DMSO according to the calibration curve obtained from DOX/DMSO solutions with different DOX concentrations. Drug loading content (LC) and encapsulation efficiency (EE) were calculated according to the following equations:

LC (%) = (weight of loaded drug/weight of drug loaded micelle) × 100%

EE (%) = (weight of loaded drug/weight of drug in feeding) × 100%

2.8. Size and morphology of nanoparticles

Dynamic light scattering (DLS) and transmission electron microscopy (TEM) were carried out to confirm the size and morphology of the blank and drug loaded nanoparticles. DLS measurements were performed at 25.0°C to record the size change by Malvern Zetasizer Nano ZS. The sample concentration was kept at 1 mg/mL. Meanwhile, TEM was performed on a Tecnai G2 F20 S-TWIN (FEI Company, USA) electron microscope at an accelerating voltage of 200 kV. An aqueous solution of sample (1 mg/mL) was dropped onto a lacy carbon coated copper grid and air-dried before morphology observation.

2.9. Stability of nanoparticles

In order to investigate the stability of nanoparticles in different media, the nanoparticles were incubated with DI water, 10% (V/V) FBS diluted with DI water, and DMEM containing 10% (V/V) FBS, respectively. And then the solutions were stored at 4.0°C for the indicated intervals followed by the DLS determination through the Malvern Zetasizer Nano ZS. Furthermore, the dilution stability of the nanoparticles was also studied in the above solvents in 1- to 500- fold dilutions at room temperature. Changes resulted from the dilutions were recorded through DLS measurements.

2.10. In vitro drug release

In vitro drug release of the hydrophobic drug DOX from LP-g-G3P nanoparticles at different pH conditions was carried out using a dialysis method. 1.00 mg of DOX loaded LP-g-G3P dispersed in 1.00 mL of PBS solution (pH 5.0, 6.8 and 7.4) was placed in a dialysis bag (MWCO 1,000 Da) and dialysed against 25 mL of corresponding buffer medium which was maintained at 37.0 ± 0.5°C in a shaking bath at 120 rpm. The experiment was done in triplicate. At predetermined time points, 1.00 mL of samples was taken out from the outer phase and equal amount of fresh corresponding buffer solution was replaced to maintain the original volume. The amount of released DOX was quantified by a calibration curve using fluorescence measurement (F-7000), and fluorescence was monitored at excitation 480 nm and emission recorded in the interval of 500-700 nm (3 mm slit).

2.11. Cell culture and cellular uptake assay

The hepatoma cell line (HepG2) was purchased from Shanghai Institute for Biological Science (Shanghai, China). HepG2 cells were cultivated in DMEM-HG medium supplemented with 10% (v/v) fetal bovine serum, 100 μg/mL streptomycin and 100 IU/mL penicillin at 37°C in the atmosphere of 5% CO_2. HepG2 cells were seeded at a density of 1×10^4 cells per well in 35 mm confocal dish (Φ=15 mm). Then the cells were treated with drug-loaded nanoparticles with final DOX concentration at 5 μg/mL in the fresh medium, and free DOX·HCl was used as a control. After incubating for 1 or 6 hours, the cells were washed three times with cold PBS and observed under confocal laser scanning microscope (CLSM, Leica TCS SP5). The observation was done with excitation and emission wavelengths of 485 nm and 595 nm, respectively. For the flow cytometry measurement, HepG2 cells were seeded into the 6-well plate at a density of 1×10^5 per well. After incubating for 24 hours at 37.0°C to achieve a confluence of 70%-80%, the cells were treated with free DOX·HCl and DOX-loaded nanoparticles (DOX concentration: 5 μg/mL) for 6 hours. The cells were then washed with PBS and collected after trypsinization followed by centrifugation at 1200 rpm for 5 min. Washing with cold PBS two more times was carried out to remove the nanoparticles which were bound to the surface of cells. Finally, the cells were suspended in 0.30 mL of PBS and measured with flow cytometry.

2.12. In vitro cytotoxicity measurements

The cytotoxicity of the blank nanoparticles, free DOX·HCl and DOX-loaded nanoparticles against HepG2 and NIH3T3 cells was measured by using CCK-8 assay. Briefly, the HepG2 and NIH3T3 cells were seeded into the 96-well plate at the density of 1×10^4 per well in 100 μL complete medium and incubated overnight. Then the cells were incubated with various concentrations of blank nanoparticles, free DOX·HCl, and DOX-loaded nanoparticles for different intervals. Next, the culture medium was removed at the indicated intervals and the cells were rinsed with PBS for three times followed by the addition of 100 μL medium containing 10% CCK-8 into each well. Finally, the absorbance of the products was measured at 450 nm using a microplate

reader after incubating for 2 hours at 37.0°C in the dark. The results were expressed as the viable percentage in relative to the untreated cells. The concentration that killed 50% cells (IC50) was calculated by the ORIGIN 9.0 software.

2.13. Statistical analysis

All experiments were repeated at least six independent samples and each measurement was performed in triplicates. Data were expressed as mean values ± standard deviation. The statistical differences between treatments groups were determined using two-way analysis of variance followed by Tukey's post-hoc test. All analyses were performed with SPSS 19.0 for Windows. In all tests, P values ≤ 0.05 were considered statistically significant.

3. Results and Discussion

3.1. Synthesis and characterisation of LP-g-G3P

An amphiphilic glycopolypeptide analogue, lactosylated pullulan-graft-arginine dendrons (LP-g-G3P), was prepared using azide-alkyne click chemistry between hydrophilic lactosylated pullulan and hydrophobic generation 3 arginine dendrons bearing Pbf and Boc groups on the periphery as shown in Fig. 1. Click chemistry has been proven as a highly efficient and convenient approach to obtain amphiphilic polysaccharides. The synthesis of alkynated peptide dendrons included the conjugation of two successive additions of L-lysine into an alkyne-containing compound followed by the addition of L-arginine bearing 8 hydrophobic protective groups. Syntheses were achieved via amide bonds formation between amine groups and carboxyl groups in the presence of powerful coupling reagents such as carbodiimide (EDCI) and HBTU. Firstly, the amine group of propargylamine was reacted with the carboxyl group of the lysine leading to alkyne-G1(K)P. Fig. 2A showed the Mass Spectra (MS) data confirming the structure of the alkyne-G1(K)P which contained 2 terminal amines protective BOC groups. For alkyne-G1(K)P (M = 383.24), the most abundant peak (m/z = 406.03) was assigned as a sodium adduct $[M + Na]^+$. To create a branched structure, another lysine was further conjugated to the terminal amine groups of G1 dendrons to lead into alkyne-G2(K)P. Arginine dendrons of generation 3, alkyne-G3(R)P,

were obtained in the similar way as that of alkyne-G2(K)P. MS was conducted to verify the products and trace any source of impurities. Alkyne-G2(K)P had the expected molecular weight, which was 840.23 corresponding to the $[M + H]^+$ (Fig. 2B). In the MS of alkyne-G3(R)P (M = 2473.27), the most abundant peak was observed at m/z = 1259.62 (Fig. 2C), which corresponds to the $[M + 2Na]^{++}$ signal, indicating that the designed alkyne-G3(R)P has been successfully synthesized. The final alkyne-G3(R)P, therefore, carries multiple hydrophobic groups (4 Boc groups and 4 Pbf groups) which combines alkyl, aromatic, and peptide dendritic hydrophobic segments at the same time.

Pullulan itself has nine hydroxyl groups per repeating unit. These hydroxyl groups can be substituted to synthesize various derivatives. To graft the hydrophobic alkyne-G3(R)P dendrons onto the hydrophilic polysaccharides by click chemistry, hydroxyl groups of pullulan were first converted into azide to obtain azidated pullulan (azido-P). And we employed a procedure for the direct azidation of pullulan with $PPh_3/CBr_4/NaN_3$. Different conditions of azidation reactions were carried out to investigate the best parameter giving a higher degree of azidation. Table 1 listed the conditions employed as well as the elemental analysis with the calculated Degree of Substitution (DS, defined here as the degree of substitution per anhydroglucose unit). As seen, 10 equivalent molar of sodium azide gave a higher conversion (77.39 %) in a condition where equimolar quantities of Ph_3P/CBr_4 were added in the presence of ice bath compared to a lower conversion (51.68%) when added at room temperature. Furthermore, Fig. 3 showed the FTIR spectrum of azido-P containing a strong C-N_3 stretching vibration at 2108 cm^{-1} which confirmed the successful synthesis of azido-P.

To achieve a liver targeted system, pullulan modification was further conducted by directly conjugating lactobionic acid onto the surface of azido-P via EDC chemistry to gain azido-lactosylated pullulan (azido-LP), which was confirmed by FTIR and ^{1}HNMR analysis. The appearance of the peak at 1746 cm^{-1} in the FTIR (Fig. 3) was the stretching vibration absorbance of C=O in ester bonds which confirmed the conjugation between carbonyl groups of the lactobionic

acid and hydroxyl groups of the pullulan. The peaks at 4.2 and 4.6 ppm in ^{1}HNMR (Fig. 4) of azido-LP were related to the H_c and H_d signals of lactobionic acid moiety, respectively. The chemical composition of lactobionic acid in azido-LP at C-6 per anhydroglucose unit was determined to be 34.45% by assigning the protons of H_b in pullulan and the proton of H_d in lactobionic acid. It should be noted that the azido-P used at this step contained 49.02% azide groups to allow more chances of lactobionic acid to be conjugated.

A classic copper-catalysed reaction was used to synthesize lactosylated pullulan graft G3(R)P copolymer (LP-g-G3P) by reacting alkyne-G3(R)P with azido-LP. The chemical structures of graft copolymers were verified by FTIR and ^{1}HNMR spectra. The click conjugation was confirmed by the disappearance of the azido group peak at 2108 cm^{-1} in azido-LP. Moreover, the ^{1}HNMR spectra of LP-g-G3P in Fig. 4 showed a signal at 7.90 ppm (H_e) indicating the triazole proton present in the 5-membered heteroatom ring formed from the click chemistry. Moreover, the graft level of G3(R)P dendrons onto the lactosylated pullulan was 18.51%, according to the integral intensities of H_h in G3(R)P and H_a in pullulan. The resulting amphiphile (LP-g-G3P) not only owned the hydrophobic blocks consisting of alkyl, aromatic and peptide dendritic moieties, but also possessed the hydrophilic lactosylated pullulan segments which have a high affinity toward liver cells.

3.2. The self-assembly and characterization of LP-g-G3P and drug loaded nanoparticles

Micellization is a general phenomenon, studied widely in the field of drug delivery to increase the bioavailability of lipophilic drugs. G3(R)P dendrons bearing 8 hydrophobic groups (4 Boc groups and 4 Pbf groups) was conjugated with the hydrophilic lactosylated pullulan to form an amphiphilic glycopolypeptide system. Owing to the amphiphilic structure of LP-g-G3P, it could self-assemble into core-shell micelles in aqueous solution, which was a good solvent for lactosylated pullulan backbone and poor solvent for G3(R)P dendrons. Fluorescence measurements were carried out in order to monitor the self-assembly behaviour of amphiphilic LP-g-G3P copolymer. The CAC of the LP-g-G3P nanoparticles was determined by fluorescence technique, using pyrene as a hydrophobic probe. As shown in Fig. 5, a lower CAC value of 8.87

ug/mL was obtained in water. The G3(R)P dendrons bearing multiple hydrophobic groups including alkyl Boc groups, phenyl Pbf groups, and peptide dendritic moieties tend to aggregate in water. They are stabilized via the strong dipolar π-π interactions between their phenyl groups, indicating greater stability of LP-g-G3P self-assemblies. It is well known that the lower the CAC value is, the higher the assembly stability is in aqueous solution (Allen et al., 1999).

DLS measurements and TEM analysis were performed on the nanoparticles solutions above the CAC, at a constant copolymer concentration of 1 mg/mL. The size and size distribution of LP-g-G3P nanoparticles in DI water presented a lower average size (54±8 nm with PDI 0.131) (Fig. 6A), possibly due to the fact that there is a higher hydrophobic effect of the multiple hydrophobic groups contributing to a tighter hydrophobic core. Moreover, TEM image (Fig. 6B) showed monodispersed, spherical nanoparticles with an average size similar to the one obtained with DLS analysis.

The amphiphilic glycopolypeptide LP-g-G3P could be used as novel nanocarriers for the application in anticancer therapy. Both lactose and pullulan could actively target asialoglycoprotein receptor (ASGPR) which are expressed on hepatocytes and hepatoma cells of the liver (Kawasaki et al., 2016; Singh et al., 2015). Therefore, LP-g-G3P nanoparticles containing hydrophilic lactosylated pullulan shell could be of great benefit for the development of liver targeted drug delivery systems. In addition, considering the highly hydrophobic core of LP-g-G3P nanoparticles, we envisioned that it might also be able to accommodate hydrophobic neutral drugs. To test this possibility, we have chosen hydrophobic neutral doxorubicin (DOX) as the model drug to study the loading, release, stability, and cytotoxicity of these core-shell nanoparticles on HepG2 or NIH3T3 cell lines. As a hydrophobic anticancer model drug, DOX was successfully entrapped physically into the hydrophobic core of LP-g-G3P nanoparticles. The hydrophobic G3(R)P dendrons bearing alkyl, aromatic and peptide dendritic moieties would have highly strong interactions with aromatic drug DOX, including π-π interactions, hydrogen bonding and hydrophobic interactions. Furthermore, such multiple interactions have the merits of enhanced

drug loading capacity, improved stability against dilution and excellent sustained-release property. The amount of entrapped DOX into LP-g-G3P nanoparticles reached 16.89% and the calculated entrapment efficiency was 56.34%. Furthermore, DLS and TEM measurements (Fig. 6C and D) showed excellent distribution of drug loaded DOX/LP-g-G3P nanoparticles in aqueous media. An increase of average size of the DOX loaded DOX/LP-g-G3P nanoparticles was observed with a mean of 68±9 nm. It has been reported that particle sizes in the range of 50-300 nm have slower removal rate from the circulation (Bae and Park, 2011). Therefore, we deduced that the size of DOX/LP-g-G3P nanoparticles would favour a good prolonged circulation due to the low uptake by the reticuloendothelial system (RES) and therefore achieve a better targeting effect by allowing more time for their interaction with the ASGPRs.

3.3. Stability of the DOX/LP-g-G3P nanoparticles

As a result of the amphiphilic structure of LP-g-G3P, it could be self-assembled into core-shell micelles in aqueous solution. To explore the long-term stability of the DOX/LP-g-G3P nanoparticles, the nanoparticles were suspended in DI water, 10% (V/V) FBS diluted with DI water, and DMEM containing 10% (V/V) FBS up to 120 hours. DLS measurement showed there were few size distribution changes in three different media as the time increased even to 120 h (Fig. 7A), which signified that these three different media had no effect on the size distribution and PDI of the DOX/LP-g-G3P nanoparticles. Furthermore, owing to the dilution that can be caused by the blood stream when the DOX/LP-g-G3P nanoparticles are injected into the body, the nanoparticles would suffer from the dissociation of self-assemblies leading to the premature release of the loaded drug. Therefore we explored the stability of the DOX/LP-g-G3P nanoparticles against dilution with three different media. As shown in Fig. 7B, there was no obvious changes in three media even after 500-fold dilution which implied the DOX/LP-g-G3P nanoparticles had good stability against dilution. The results implied that the DOX/LP-g-G3P nanoparticles had good stability that met the requirements of the drug delivery and they could remain stable before internalization by cells.

3.4. In vitro drug release studies of the DOX/LP-g-G3P nanoparticles

In this study, the ability of the LP-g-G3P nanoparticles acting as drug delivery systems was preliminary evaluated. An important aspect in using nanoparticles as drug delivery systems is the effect on the drug release behaviour. The pH change occurs at many specific or physiological sites in the body, for example, the tumor extracellular environment is more acidic (~pH 6.8) than blood and normal tissues (pH 7.4), and the pH values of endosome and lysosome are even lower at 5.0~5.5. Therefore, the release of DOX from DOX/LP-g-G3P nanoparticles was investigated at different pH (5.0, 6.8 and 7.4) conditions. As illustrated in Fig. 8, the DOX/LP-g-G3P nanoparticles had brought about approximately 6 wt% of DOX released at pH 7.4 after 62 hours, which confirmed the stability of the DOX/LP-g-G3P nanoparticles and a low premature drug release in a physiological pH condition (mimicking the blood circulation). This was possibly explained by the fact that G3(R)P dendrons with multiple hydrophobic groups presented in the core of LP-g-G3P nanoparticles would have highly strong interactions with DOX, including π-π interactions, hydrogen bonding and hydrophobic interactions.

The DOX release rate was increased along with the decrease of pH value. The cumulative release of DOX showed only a slight increase and reached to 10 wt% at pH 6.8 at the same time scale. In an acidic pH condition (pH 5.0, mimicking endo/lysosomal condition), however, the DOX drug release was much faster than in a physiological pH as it showed a faster release to reach over 25 wt% within 10 hours, continued a sustained release to reach almost 40 wt% after 62 hours. In vitro sustained release behaviour of DOX from DOX/LP-g-G3P nanoparticles could be the advantageous feature in therapy: the primary high drug release (25 wt% within 10 hours) provides an initial dose, followed by a sustained release. The driving force for the release of DOX from DOX/LP-g-G3P nanoparticles could be ascribed to protonation of the amine group in DOX with hydrophilicity enhancement at lower pH values and diffusion through the hydrophilic lactosylated pullulan shell. The initial fast release of DOX from DOX/LP-g-G3P nanoparticles could be

reasonably explained by the fact that a certain amount of DOX loaded in the centre of the hydrophobic core may quickly respond to the change of pH value and preferentially diffuse through the lactosylated pullulan shell. Whereas some DOX highly interacting with the hydrophobic G3(R)P dendrons would protonate slowly, causing a sustained release.

3.5. Analysis of cellular internalization

Lactose and pullulan were chosen to construct the hydrophilic block of the amphiphilic glycopolypeptide LP-g-G3P as recognition of sugars due to their well-known ability to bind hepatic lectins, such as ricinus communis agglutinin I (RCA_{120}) and asialoglycoprotein receptor (ASGPR) of hepatocytes. It is likely that lactosylated pullulan served as the hydrophilic shell of LP-g-G3P nanoparticles could facilitate liver targeted delivery. In order to preliminarily investigate the cellular internalization efficiency of the DOX/LP-g-G3P nanoparticles, confocal laser scanning microscopy and flow cytometry were performed. HepG2 cell line used for internalization study of DOX/LP-g-G3P nanoparticles expressed both ASGPRs and RCA_{120} (Satoh et al., 2007; Singh et al., 2015). Free hydrophilic DOX·HCl solution and DOX/LP-g-G3P nanoparticles with an equivalent amount of DOX (5 μg/mL) were added to exponentially growing cells for 1 or 6 hours. As presented in Fig. 9A, after 6 hours of incubation, both DOX·HCl solution and DOX/LP-g-G3P nanoparticles treated cells exhibited strong red signals. However, drug intracellular distribution of the DOX/LP-g-G3P nanoparticles is quite different from that of the DOX·HCl solution. Because of the hydrophilic nature of the DOX·HCl, it could penetrate the cell membrane unselectively through a diffusion mechanism. For DOX·HCl treated cells, strong red fluorescence was observed in cell nuclei in addition to a very weak fluorescence in the cytoplasm, indicating rapid intercalation of intracellular DOX·HCl to the chromosomal DNA after passive diffusion into the cells. On the other hand, HepG2 cells treated with DOX/LP-g-G3P nanoparticles showed speckled red dots throughout the cytoplasm, revealing that DOX/LP-g-G3P nanoparticles were initially trapped within endosomal compartments after cellular uptake. These phenomena not only demonstrated that DOX/LP-g-G3P nanoparticles could efficiently transport hydrophobic

DOX into the cytoplasm, but also suggested that the internalization mechanism of DOX/LP-g-G3P nanoparticles was quite different from that of hydrophilic free DOX·HCl. Thus, we could conclude that DOX/LP-g-G3P nanoparticles were internalized by HepG2 cells mainly via an endocytic pathway and were then localized in acidic endo/lysosomes. DOX was released from LP-g-G3P nanoparticles in a sustained manner from inside endo/lysosomes because the in vitro DOX release of DOX/LP-g-G3P nanoparticles was a relatively slow process even at pH 5.0 condition (Fig. 8).

Since DOX itself is fluorescent, fluorescence intensity is directly proportional to the amount of DOX internalized. Therefore, flow cytometry has been used for quantitative determination of DOX uptake in cells. HepG2 cells were incubated with free DOX·HCl and DOX/LP-g-G3P nanoparticles solutions with equivalent DOX concentration for 6 hours. Cells without any DOX treatment were used as a negative control. The results shown in Fig. 9B also indicated that the hydrophobic DOX was successfully transported into cells by being loaded in LP-g-G3P nanoparticles. The cellular uptake of DOX/LP-g-G3P nanoparticles could reach to the level of those treated with free DOX·HCl solution. Taken together, LP-g-G3P nanoparticles have higher affinity toward liver due to presence of lectin like receptors on HepG2 cells, which possess biological affinity for sugar residues. LP-g-G3P nanoparticles with lectins undergo endocytosis and get internalized with high affinity to the HepG2 cells.

3.6. In vitro antitumor effect of DOX/LP-g-G3P nanoparticles

In order to investigate in vitro cytotoxicity of blank LP-g-G3P nanoparticles and in vitro antitumor effect of drug-loaded DOX/LP-g-G3P nanoparticles, the CCK-8 assay was performed. Blank LP-g-G3P nanoparticles were applied in both HepG2 and NIH3T3 cell lines at concentrations ranging from 1 to 200 μg/mL for 24 hours and the effect on cell viability was measured and showed in Fig. 10. For the blank LP-g-G3P nanoparticles themselves, there was no significant cytotoxicity (viabilities remained above 90%) even for the polymer concentration up

to 200 μg/mL in both HepG2 and NIH3T3 cells which implied the glycopolypeptide LP-g-G3P had excellent biocompatibility.

To value the dose-dependent effect of DOX on the viability of HepG2 and NIH3T3 cells, the immediate effect after the end of DOX treatment was performed through CCK-8 assay. HepG2 and NIH3T3 cells were ASGPRs and RCA_{120} positive and negative cells, respectively. Cytotoxicity was concentration dependent and increased with increasing DOX concentration for both free DOX·HCl solution and DOX/LP-g-G3P nanoparticles in HepG2 and NIH3T3 cells (Fig. 11A and 11B). Similarly, the IC50 (the concentration that caused 50% cell death) value was also obtained with DOX concentration varied from 0.001 to 100 μg/mL. The IC50 of free DOX·HCl solution and DOX/LP-g-G3P nanoparticles were calculated to be 0.046 μg/mL and 0.675 μg/mL respectively in HepG2 cells, while 0.129 μg/mL and 1.701 μg/mL in NIH3T3 cells separately.

The IC50 value of DOX/LP-g-G3P nanoparticles was higher than that of free DOX·HCl solution (Fig. 11A and 11B) despite similar amounts of internalized DOX (Fig. 9). These observations might be due to the fact that hydrophilic DOX·HCl could be easily transported into the cells and accumulated rapidly in nuclei, whereas hydrophobic DOX loaded LP-g-G3P nanoparticles may be internalized by endocytosis followed by the disassembly of the nanoparticles, releasing DOX from cytosolic compartments in a sustained manner and continuously producing more cytotoxicity after incubation. From this standpoint, the delay effect (Eliaz et al., 2004) (after DOX removal from the medium) of DOX/LP-g-G3P nanoparticles may perform better than its immediate effect. Fig. 11C showed that the cytotoxicity of the DOX/LP-g-G3P nanoparticles in HepG2 cells at different concentrations and varying time, the cell viability could decrease with increasing DOX concentration and incubation time. It could also be seen that the IC50 values after 1, 2, 3 and 4 days were 0.675, 0.507, 0.242 and 0.160 μg/mL respectively, which implied the cytotoxicity of the DOX/LP-g-G3P nanoparticles had time-dependent effects.

Furthermore, It was noteworthy that the IC50 of DOX/LP-g-G3P nanoparticles in NIH3T3 cells was higher than that in HepG2 cells (Fig. 11A and 11B), which implied that the DOX/LP-g-

G3P nanoparticles had a better affinity toward the HepG2 cells. Meanwhile, the cytotoxicity of the DOX/LP-g-G3P nanoparticles with 0.5 μg/mL DOX concentration at varying time in both HepG2 cells and NIH3T3 cells was also tested as Fig. 11D showed. It could be seen that the cell viability of DOX/LP-g-G3P nanoparticles after 1, 2, 3 and 4 days in NIH3T3 cells at every indicated time point was higher than that of HepG2 cells, which also indicated that the DOX/LP-g-G3P nanoparticles had a better affinity toward the HepG2 cells and could kill the tumor cells, but were less toxic to normal cells.

4. Conclusions

In summary, we have developed an original amphiphilic glycopolypeptide analogue, lactosylated pullulan-graft-arginine dendrons (LP-g-G3P), using azide-alkyne click chemistry between hydrophilic lactosylated pullulan and hydrophobic generation 3 arginine dendrons bearing Pbf and Boc groups on the periphery. The resulting amphiphile LP-g-G3P not only owned the hydrophobic blocks consisting of alkyl, aromatic and peptide dendritic moieties, but also possessed the hydrophilic lactosylated pullulan segments which have a high affinity toward liver cells. LP-g-G3P could form core-shell nanoassemblies with an average diameter about 54 nm by the fine-tuning of intra- and intermolecular interactions and could also provide a safe and spacious harbor for the hydrophobic drugs. The polyaromatic anticancer drug (DOX) would have highly strong interactions with hydrophobic G3(R)P dendrons, including π-π interactions, hydrogen bonding and hydrophobic interactions. Such multiple interactions have the merits of enhanced drug loading capacity, improved stability against dilution, and excellent sustained release property. Blank LP-g-G3P nanoparticles exhibited an excellent biocompatibility both in the normal and tumor cells, whereas DOX loaded LP-g-G3P nanoparticles could be effectively internalized into the hepatoma carcinoma cells and dramatically inhibited cell proliferation. Thus, this study presents a straightforward and versatile way to develop amphiphilic and biofunctional glycopolypeptide-based drug delivery systems.

Acknowledgements

This work was financially supported by National Natural Science Foundation of China (NSFC, 81361140343, 81621003 and 31500810), International Science and Technology Cooperation Program of China (2015DFE52780), and the European Commission Research and Innovation (PIRSES-GA-2011-295218). The authors are grateful to the Young Scholar Program of Sichuan University (2015SCU11038) and the Foundation for Talent Introduction from Sichuan University (YJ201464).

References

Akhlaghi, S.P., Peng, B., Yao, Z., Tam, K.C., 2013. Sustainable nanomaterials derived from polysaccharides and amphiphilic compounds. Soft Matter 9, 7905-7918.

Allen, C., Maysinger, D., Eisenberg, A., 1999. Nano-engineering block copolymer aggregates for drug delivery. Colloids Surf., B 16, 3-27.

Alvarez-Lorenzo, C., Blanco-Fernandez, B., Puga, A.M., Concheiro, A., 2013. Crosslinked ionic polysaccharides for stimuli-sensitive drug delivery. Adv. Drug Delivery Rev. 65, 1148-1171.

Aschenbrenner, E., Bley, K., Koynov, K., Makowski, M., Kappl, M., Landfester, K., Weiss, C.K., 2013. Using the polymeric ouzo effect for the preparation of polysaccharide-based nanoparticles. Langmuir 29, 8845-8855.

Börner, H.G., 2009. Strategies exploiting functions and self-assembly properties of bioconjugates for polymer and materials sciences. Prog. Polym. Sci. 34, 811-851.

Bae, Y.H., Park, K., 2011. Targeted drug delivery to tumors: Myths, reality and possibility. J. Controlled Release 153, 198-205.

Bravo-Osuna, I., Vauthier, C., Farabollini, A., Palmieri, G.F., Ponchel, G., 2007. Mucoadhesion mechanism of chitosan and thiolated chitosan-poly(isobutyl cyanoacrylate) core-shell nanoparticles. Biomaterials 28, 2233-2243.

Cao, Y., Gu, Y., Ma, H., Bai, J., Liu, L., Zhao, P., He, H., 2010. Self-assembled nanoparticle drug delivery systems from galactosylated polysaccharide–doxorubicin conjugate loaded doxorubicin. Int. J. Biol. Macromol. 46, 245-249.

Carlini, A.S., Adamiak, L., Gianneschi, N.C., 2016. Biosynthetic polymers as functional materials. Macromolecules 49, 4379-4394.

Chandel, A.K.S., Bera, A., Nutan, B., Jewrajka, S.K., 2016. Reactive compatibilizer mediated precise synthesis and application of stimuli responsive polysaccharides-polycaprolactone amphiphilic co-network gels. Polymer 99, 470-479.

Dupayage, L., Nouvel, C., Six, J.L., 2011. Protected versus unprotected dextran macroinitiators for atrp synthesis of dex-g-pmma. J. Polym. Sci., Part A: Polym. Chem. 49, 35-46.

Dupayage, L., Save, M., Dellacherie, E., Nouvel, C., Six, J.-L., 2008. Pmma-grafted dextran glycopolymers by atom transfer radical polymerization. J. Polym. Sci., Part A: Polym. Chem. 46, 7606-7620.

Eliaz, R.E., Nir, S., Marty, C., Szoka, F.C., 2004. Determination and modeling of kinetics of cancer cell killing by doxorubicin and doxorubicin encapsulated in targeted liposomes. Cancer Res. 64, 711-718.

Gu, C., Le, V., Lang, M., Liu, J., 2014. Preparation of polysaccharide derivates chitosan-graft-poly(varepsilon-caprolactone) amphiphilic copolymer micelles for 5-fluorouracil drug delivery. Colloids Surf., B 116, 745-750.

Hassan, M.L., Moorefield, C.N., Newkome, G.R., 2004. Regioselective dendritic functionalization of cellulose. Macromol. Rapid Commun. 25, 1999-2002.

Hassani, L.N., Hendra, F., Bouchemal, K., 2012. Auto-associative amphiphilic polysaccharides as drug delivery systems. Drug Discovery Today 17, 608-614.

Kawasaki, R., Sasaki, Y., Katagiri, K., Mukai, S.-a., Sawada, S.-i., Akiyoshi, K., 2016. Magnetically guided protein transduction by hybrid nanogel chaperones with iron oxide nanoparticles. Angew. Chem. Int. Ed. 55, 11377-11381.

Li, H., Xu, X., Li, Y., Geng, Y., He, B., Gu, Z., 2013. Design and self-assembly of amphiphilic peptide dendron-jacketed polysaccharide polymers into available nanomaterials. Polym. Chem. 4, 2235-2238.

Li, J., Huo, M., Wang, J., Zhou, J., Mohammad, J.M., Zhang, Y., Zhu, Q., Waddad, A.Y., Zhang, Q., 2012. Redox-sensitive micelles self-assembled from amphiphilic hyaluronic acid-deoxycholic acid conjugates for targeted intracellular delivery of paclitaxel. Biomaterials 33, 2310-2320.

Liu, Y., Sun, J., Zhang, P., He, Z., 2011. Amphiphilic polysaccharide-hydrophobicized graft polymeric micelles for drug delivery nanosystems. Curr. Med. Chem. 18, 2638-2648.

Luo, K., Li, C., Li, L., She, W., Wang, G., Gu, Z., 2012. Arginine functionalized peptide dendrimers as potential gene delivery vehicles. Biomaterials 33, 4917-4927.

Majoinen, J., Haataja, J.S., Appelhans, D., Lederer, A., Olszewska, A., Seitsonen, J., Aseyev, V., Kontturi, E., Rosilo, H., Österberg, M., Houbenov, N., Ikkala, O., 2014. Supracolloidal multivalent interactions and wrapping of dendronized glycopolymers on native cellulose nanocrystals. J. Am. Chem. Soc. 136, 866-869.

Nichifor, M., Mocanu, G., Stanciu, M.C., 2014. Micelle-like association of polysaccharides with hydrophobic end groups. Carbohydr. Polym. 110, 209-218.

Percec, V., Dulcey, A.E., Balagurusamy, V.S.K., Miura, Y., Smidrkal, J., Peterca, M., Nummelin, S., Edlund, U., Hudson, S.D., Heiney, P.A., Duan, H., Magonov, S.N., Vinogradov, S.A., 2004. Self-assembly of amphiphilic dendritic dipeptides into helical pores. Nature 430, 764-768.

Pramod, P.S., Takamura, K., Chaphekar, S., Balasubramanian, N., Jayakannan, M., 2012. Dextran vesicular carriers for dual encapsulation of hydrophilic and hydrophobic molecules and delivery into cells. Biomacromolecules 13, 3627-3640.

Qiu, H., Hudson, Z.M., Winnik, M.A., Manners, I., 2015. Multidimensional hierarchical self-assembly of amphiphilic cylindrical block comicelles. Science 347, 1329-1332.

Rösler, A., Vandermeulen, G.W.M., Klok, H.-A., 2012. Advanced drug delivery devices via self-assembly of amphiphilic block copolymers. Adv. Drug Delivery Rev. 64, 270-279.

Roglin, L., Lempens, E.H., Meijer, E.W., 2011. A synthetic "tour de force": Well-defined multivalent and multimodal dendritic structures for biomedical applications. Angew. Chem. Int. Ed. Engl. 50, 102-112.

Rosen, B.M., Wilson, C.J., Wilson, D.A., Peterca, M., Imam, M.R., Percec, V., 2009. Dendron-mediated self-assembly, disassembly, and self-organization of complex systems. Chem. Rev. 109, 6275-6540.

Saravanakumar, G., Jo, D.G., H. Park, J., 2012. Polysaccharide-based nanoparticles: A versatile platform for drug delivery and biomedical imaging. Curr. Med. Chem. 19, 3212-3229.

Satoh, T., Kakimoto, S., Kano, H., Nakatani, M., Shinkai, S., Nagasaki, T., 2007. In vitro gene delivery to hepg2 cells using galactosylated 6-amino-6-deoxychitosan as a DNA carrier. Carbohydr. Res. 342, 1427-1433.

Singh, R.S., Kaur, N., Kennedy, J.F., 2015. Pullulan and pullulan derivatives as promising biomolecules for drug and gene targeting. Carbohydr. Polym. 123, 190-207.

Takahashi, H., Sawada, S.-i., Akiyoshi, K., 2011. Amphiphilic polysaccharide nanoballs: A new building block for nanogel biomedical engineering and artificial chaperones. ACS Nano 5, 337-345.

Wang, C., Wang, Z., Zhang, X., 2012. Amphiphilic building blocks for self-assembly: From amphiphiles to supra-amphiphiles. Acc. Chem. Res. 45, 608-618.

Wang, J.J., Zeng, Z.W., Xiao, R.Z., Xie, T., Zhou, G.L., Zhan, X.R., Wang, S.L., 2011. Recent advances of chitosan nanoparticles as drug carriers. Int. J. Nanomedicine 6, 765-774.

Xu, W., Ding, J., Xiao, C., Li, L., Zhuang, X., Chen, X., 2015. Versatile preparation of intracellular-acidity-sensitive oxime-linked polysaccharide-doxorubicin conjugate for malignancy therapeutic. Biomaterials 54, 72-86.

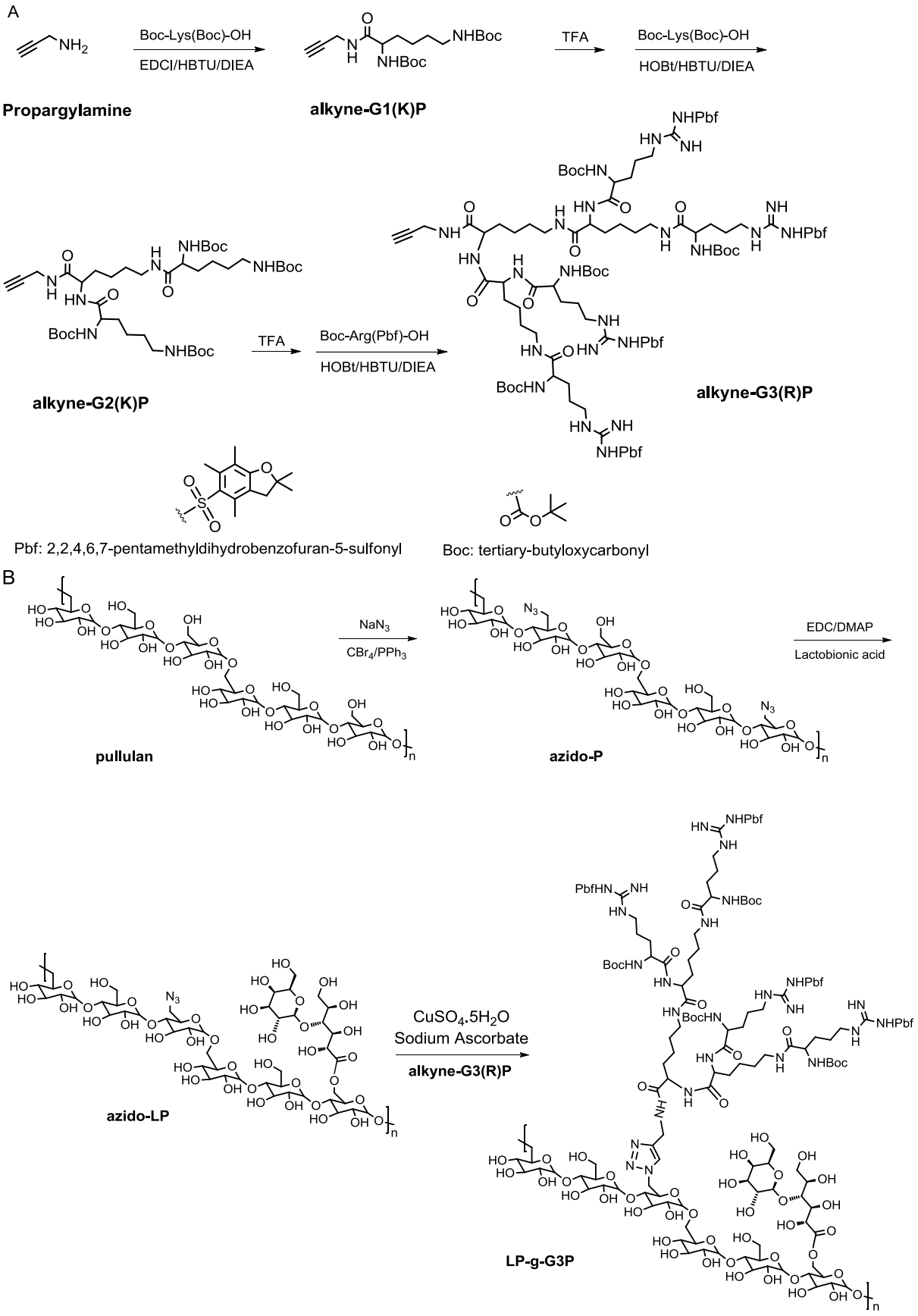

Fig. 1. (A) Synthesis routes to alkyne-G3(R)P, and (B) Reaction schemes of the amphiphilic LP-g-G3P.

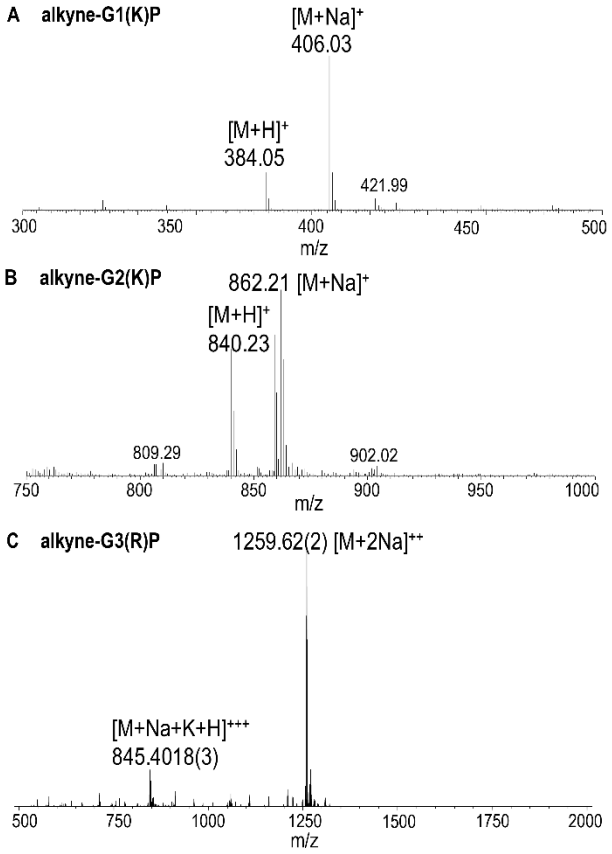

Fig. 2. Mass spectra of (A) alkyne-G1(K)P, (B) alkyne-G2(K)P, and (C) alkyne-G3(R)P.

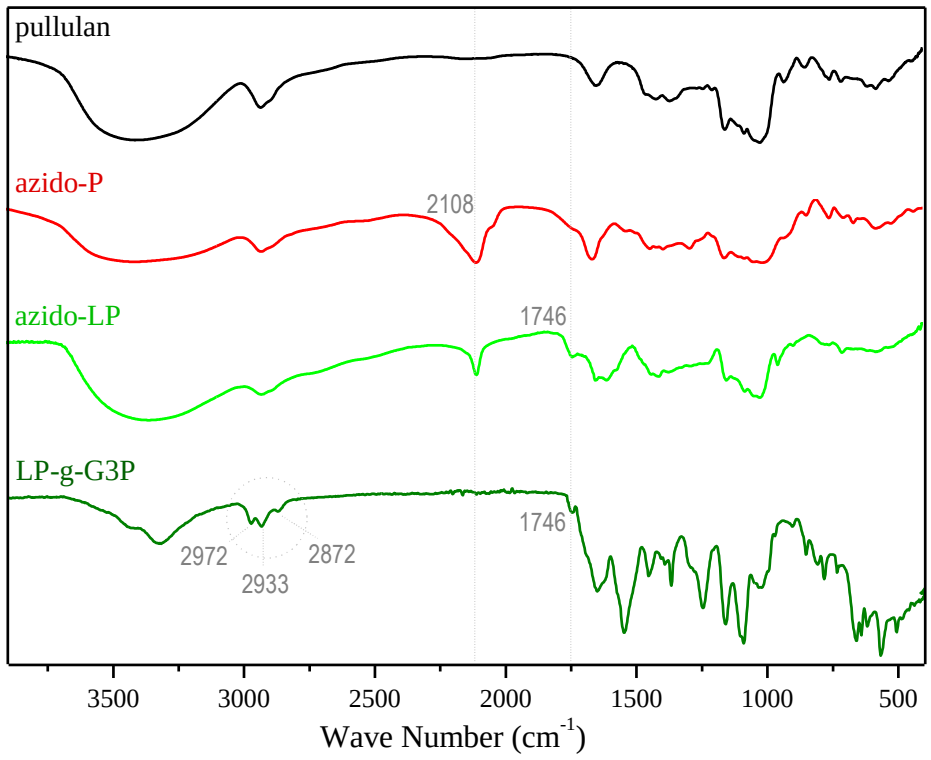

Fig. 3. FTIR spectra of pullulan, azido-P, azido-LP, and LP-g-G3P.

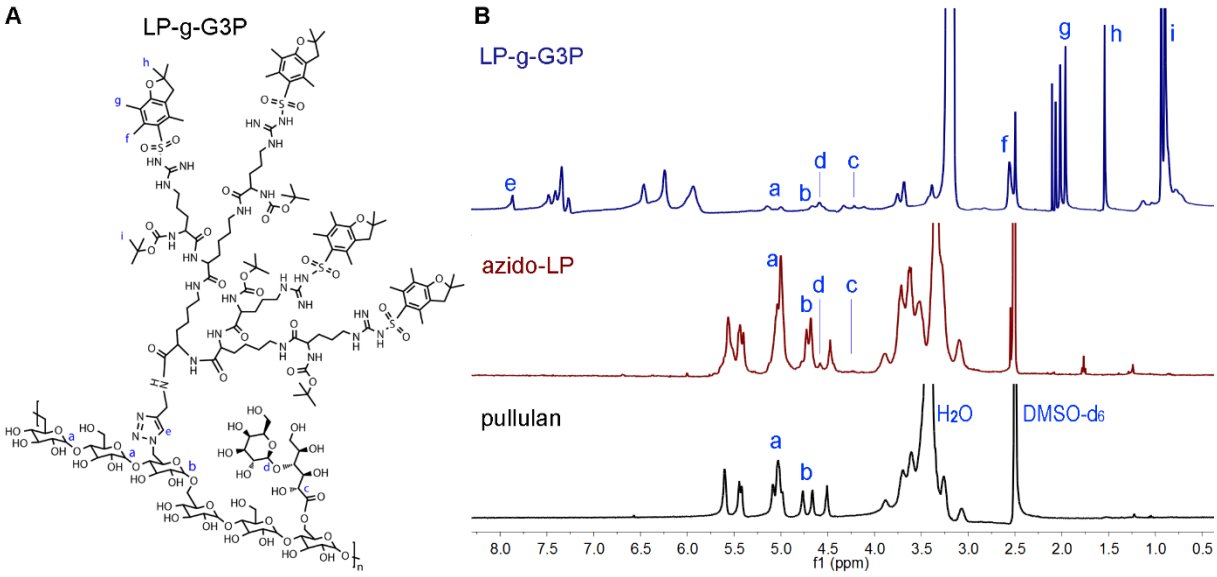

Fig. 4. (A) Chemical structure of LP-g-G3P, and (B) ^{1}HNMR (400 MHz, DMSO-d_6) of pullulan, azido-LP and LP-g-G3P.

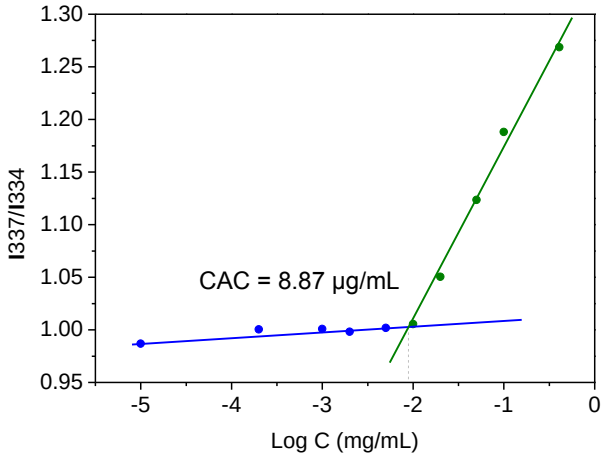

Fig. 5. Critical association concentration of LP-g-G3P measured using the fluorescent dye pyrene.

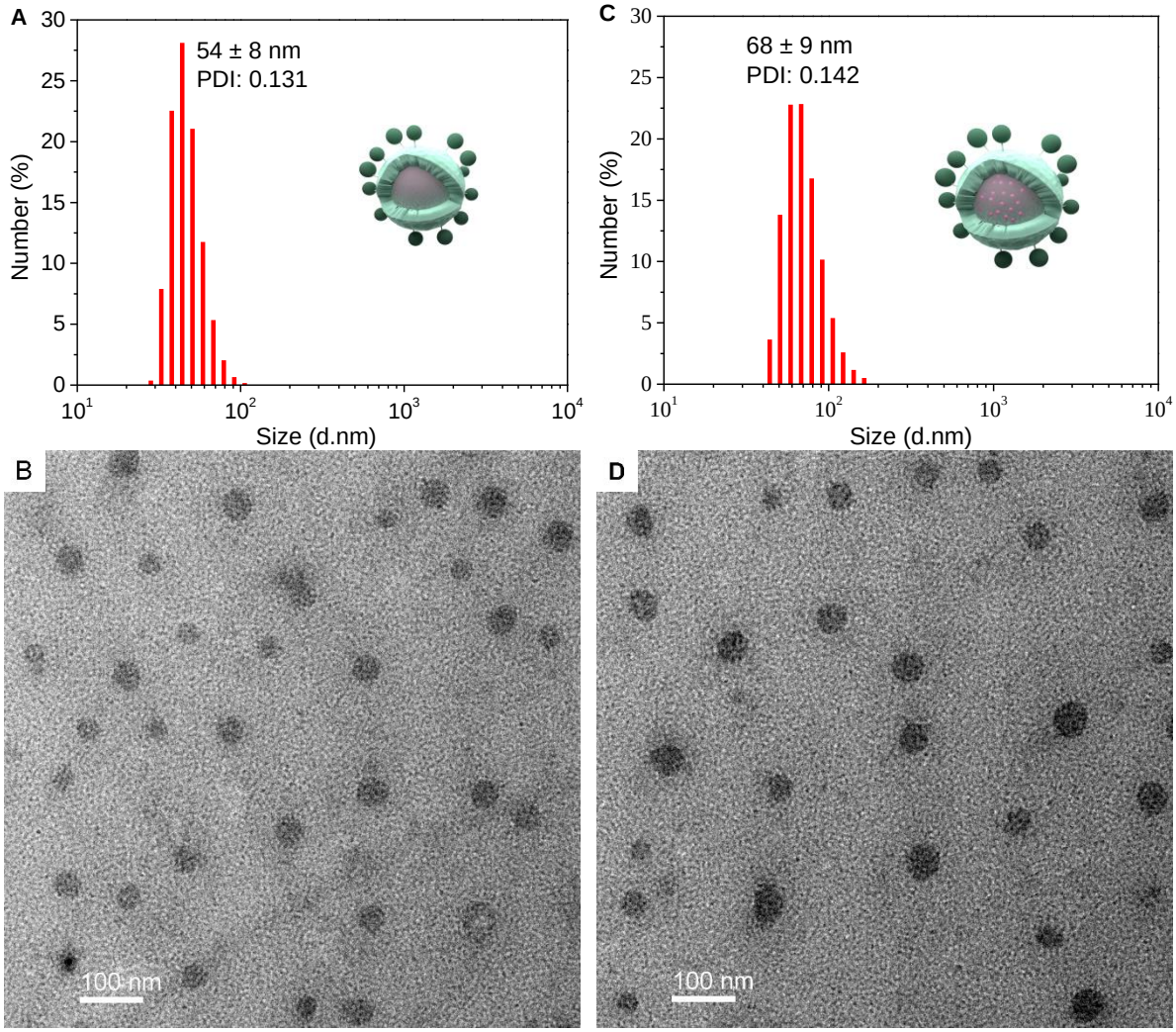

Fig. 6. Size distribution and morphology studies of LP-g-G3P nanoparticles (A, B) and DOX loaded LP-g-G3P nanoparticles (C, D) by Dynamic light scattering and Transmission electron microscopy.

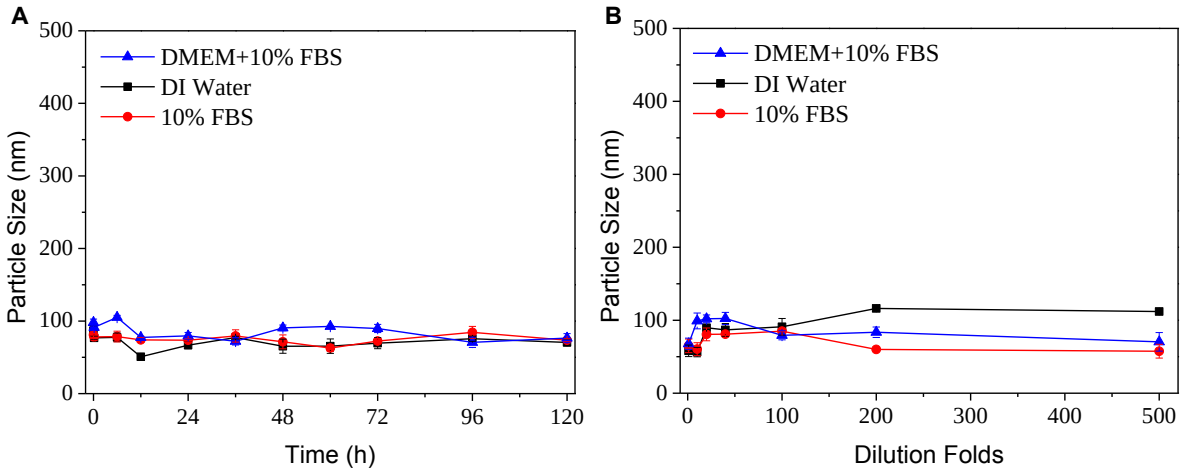

Fig. 7. (A) DLS results of DOX/LP-g-G3P nanoparticles after long time incubation in DI water, 10% (V/V) FBS and DMEM containing 10% (V/V) FBS, respectively. (B) Particle size changes of DOX/LP-g-G3P nanoparticles after dilution of different times with DI water, 10% (V/V) FBS and DMEM containing 10% (V/V) FBS, respectively.

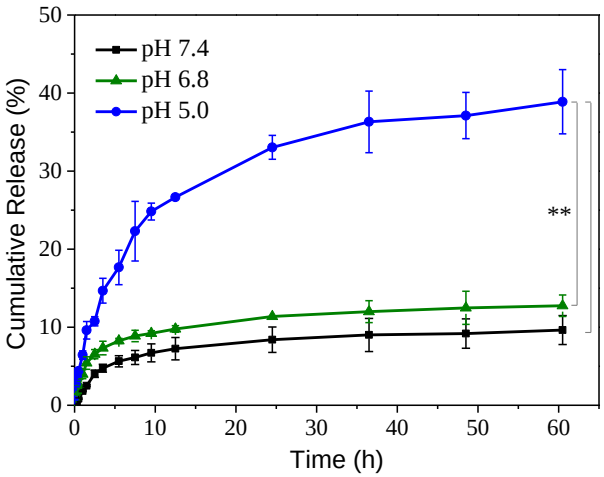

Fig. 8. *In vitro* drug release profile of DOX loaded LP-g-G3P nanoparticles under different pH condition (pH 7.4, 6.8 and 5.0) at 37°C (n = 6, $^{**}p < 0.05$ by two-way ANOVA, followed by Tukey's post-hoc test).

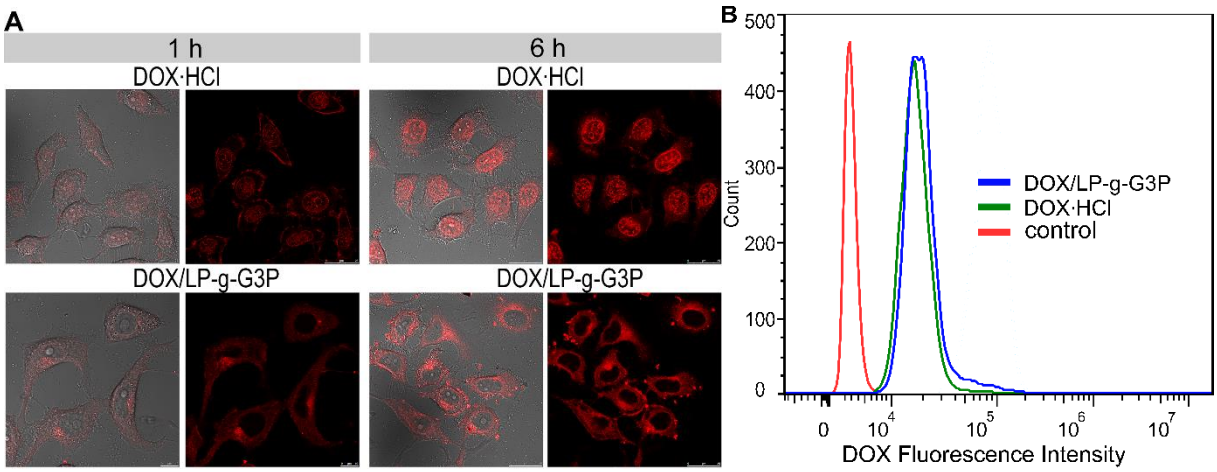

Fig. 9. (A) Fluorescence microscopy images of the HepG2 cells incubated with DOX/LP-g-G3P nanoparticles and free DOX·HCl for 1 and 6 hours. (B) Flow cytometry histogram of HepG2 cells incubated with DOX/LP-g-G3P nanoparticles and free DOX·HCl for 6 hours.

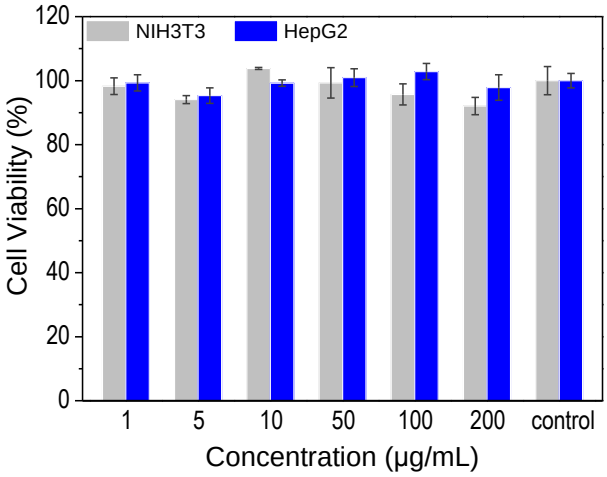

Fig. 10. Biocompatibility assay of HepG2 and NIH3T3 cells against blank LP-g-G3P nanoparticles for 24 hours.

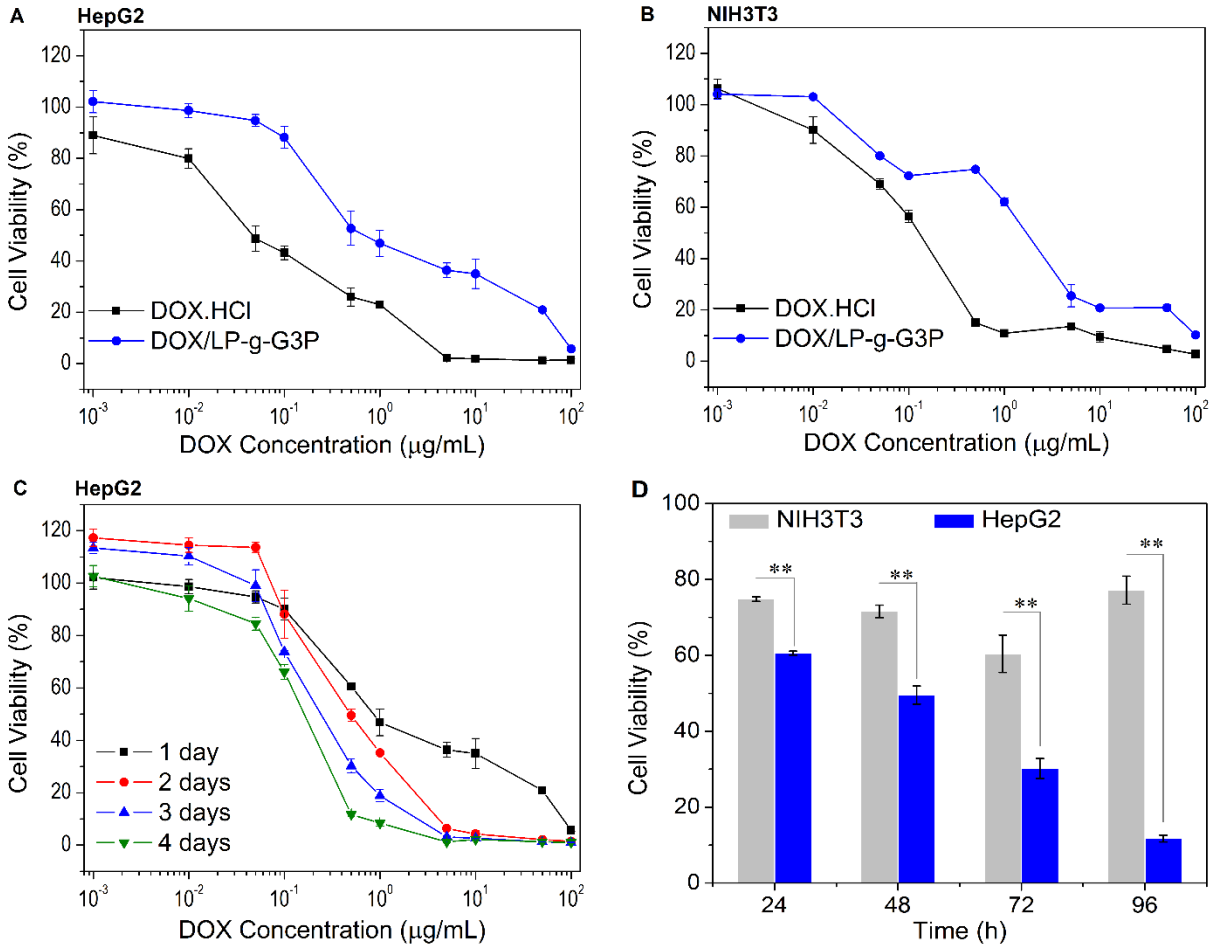

Fig. 11. Dose dependent cytotoxicity of (A) HepG2 and (B) NIH3T3 cells against DOX loaded LP-g-G3P nanoparticles and free DOX·HCl solutions for 24 hours. (C) Enhanced cytotoxicity of the DOX loaded LP-g-G3P nanoparticles in HepG2 cells for varied time periods. (D) Cell viability against HepG2 and NIH3T3 cells incubated with the DOX loaded LP-g-G3P nanoparticles at the DOX equivalent 0.5 μg/mL for different time intervals (n = 6, $^{**}p < 0.05$ by two-way ANOVA, followed by Tukey's post-hoc test).

Table 1
Determination of the substitution degree of azido-P by elemental analysis.

	pullulan:NaN_3 (temperature)	C (%)	H (%)	N (%)	DS (% per unit)
pullulan	-	40.33	6.66	-	-
azido-P(1)	1: 10 (RT)	39.34	5.68	11.86	155.04%
azido-P(2)	1:10 (0°C)	32.94	5.62	14.87	232.16%
azido-P(3)	1:9 (0°C)	39.51	6.67	5.93	77.19%
azido-P(4)	1:8 (0°C)	39.24	6.56	3.74	49.02%